Appl. Phys. B 78, 895–899 (2004)
DOI: 10.1007/s00340-004-1433-6

Applied Physics B
Lasers and Optics

Invited paper

M. SCHNÜRER[1,✉]
S. TER-AVETISYAN[1,2]
S. BUSCH[1]
M.P. KALACHNIKOV[1]
E. RISSE[1]
W. SANDNER[1]
P.V. NICKLES[1]

MeV – proton emission from ultrafast laser-driven microparticles

[1] Max-Born-Institute for Nonlinear Optics and Short Pulse Spectroscopy, Max-Born-Straße 2a, 12489 Berlin, Germany
[2] Institute for Physical Research, Ashtarak-2, 378410, Armenia

Received: 30 October 2003 / Revised version: 9 January 2004
Published online: 12 March 2004 •

ABSTRACT Propagation of a high intensity ($\sim 10^{19}$ W/cm^2) ultrashort (~ 35 fs) laser pulse through a cloud of water spheres (150 nm diameter) results in hot electron driven proton acceleration up to 1 MeV. It is suggested that during the propagation of the short pulse through the low density wing of the cloud, the leading pulse pedestal is reduced owing to absorption by the preplasma created. Then, the high-intensity peak of the pulse propagates through this underdense plasma and interacts with the high-density inner part of the cloud, which has not been transformed into an underdense plasma so that a sheath acceleration process at each individual microsphere can take place. The observed proton spectra show strong modulations, which are interpreted within the framework of a known fluid-expansion model incorporating two hot-electron populations with significantly different densities and temperatures.

PACS 52.50.Jm; 52.38.Kd; 41.75.Jv

1 Introduction

Conversion of a significant part of laser energy into kinetic energy of fast ions is one of the most striking features obtained in relativistic laser interaction with dense matter. Especially, proton beams with particle energies of several MeV have a large potential for imaging of dense plasmas [1]. Further possible applications such as techniques using nuclear activated samples [2, 3] rely on proton energy and average beam flux. Up to now an optimized laser–target concept in terms of laser energy consumption cannot be given. This motivates further investigation of the underlying processes of ion acceleration with lasers. Besides intense-laser interaction with foils [4–13] having thicknesses of several microns or tens of microns, no other target concept could be demonstrated to be capable of proton emission with energies in excess of several MeV. Spherical water-droplet targets have been used recently to generate protons and deuterons with MeV energy [14, 15]. Emission of energetic protons with energies up to 1 MeV could be achieved from thin foils having an extension of about 0.1 micron [5]. It is worthwhile to irradiate smaller and less massive targets because the intense laser field can directly excite all atoms if the target is smaller than its skin depth at the laser frequency. In this case, for sufficiently high laser intensity, Coulomb explosion [16] results. Clusters, which are one kind of such ensembles, have been intensively studied (see e.g., [16]) and highly charged ions with MeV-energy (see e.g., [17]) have been produced. Besides Coulomb explosion, the space charge of the energetic electrons confined to the cluster plays an important role in driving the hydrodynamic expansion [16] provided the cluster is large. Both effects efficiently transfer laser energy into kinetic energy of the ions. Simulations in laser fields above 10^{20} W/cm^2 [18], for large clusters, yield cluster charges large enough to generate protons with MeV-energies–higher than achieved by cluster explosion until now.

In this paper, we report on interaction studies of a cloud of water microspheres (diameter ~ 150 nm) with ultrashort intense laser pulses, particularly with regard to energetic-proton emission. To our knowledge, this is the first experimental demonstration of MeV-proton emission from laser-driven micro-objects that are definitely smaller than the incident-laser wavelength. Here, a low-debris water-spray target system is exposed to laser pulses (35 fs, 600 mJ) that are about3 to 10 times shorter and have an energy 10 to 40 times lower than used in previous proton-generation experiments from solid thick foil targets [9, 11]. These experiments demonstrated proton-beam generation with particle energies in excess of 10 MeV. Similar laser parameters as used here have been also applied to foils [10, 12, 13] and to single water droplets [14, 15], giving maximum proton energies in the 1–2 MeV range. The spray target opens new aspects in laser-plasma physics because it extends the parameter range of cluster sources, especially of those from hydrogen and deuterium, which need cryogenic valve techniques [19] for the large cluster sizes desired.

2 Experimental

The experiments have been carried out with 35-fs laser pulses at 815-nm center wavelength from the MBI High-Field Ti : Sa-laser [20]. For the present experiments, pulses with energies up to 600 mJ and a beam of 70 mm diameter are focused by a $f/2.5°$ff-axis parabolic mirror. Interaction intensities of $\sim 10^{19}$ W/cm^2 have been estimated from the energy content in a focal area with a diameter of ~ 6 μm. Measurements with a third-order correlate showed a temporal contrast

✉ Fax: +49-30/6392-1329, E-mail: schnuerer@mbi-berlin.de

of our amplified Ti : Sa laser pulses at $\sim 10^{-7}$ of the pulse peak in its 1–2 ns extended pedestal. A newly developed pulsed water spray is used as target source. It is based on the expansion of superheated water through a nozzle into vacuum. Detailed characterization of the spray [21] gave a number density of droplets near the nozzle of 10^{11} droplets/cm^3 for a droplet diameter estimated at 0.15 μm. The mean atomic density near the nozzle is $> 10^{18}$ atoms/cm^3. The laser is focused at about 1 mm below the jet nozzle outlet. For this study, two identical Thomson parabola spectrometers registered the ion emission at observation angles of 0 (laser propagation direction), and 135 degrees. The spectrometer entrance pinholes have a diameter of 200 μm in a lead plate of 1 mm thickness and are placed at a distance of 35 cm from the source. Either CR-39 plates [22] or microchannel-plates were used for ion detection. The phosphorous screen of the MCP was imaged with a cooled CCD-camera. The single-particle response of this detection system was evaluated with alpha-particle emission from a Am241-source. Typically a magnetic field of about 0.27 T and electric fields of (2–6 kV/cm) have been applied.

3 Results and discussion

3.1 *Laser-pulse interaction with a spray*

Figure 1 depicts ion-spectra recorded on CR-39 plates from the spray source at 0 degrees and 135 degrees in comparison with a single-droplet source [14] (15 microns in diameter) irradiated with similar laser parameters. Proton and ion (O^{1+}) traces extend up to similar cutoff energies. For the spray, ion emission is more pronounced along the laser-propagation direction, in contrast to the single droplet where an enhanced signal in number density (and, slightly, in cut-off energy) [14] is visible in 135-degree emission. Several small micro-spheres in the spray are excited along the laser-beam propagation, which enhances the source brightness in forward direction (0 degree) in comparison with the backward direction (135 degree). Because the ions are produced inside the spray-target, they have to penetrate the surrounding target material, which leads to absorption. This effect is clearly visible in the bleaching of the proton-trace at lower energies and in the complete absorption of low-energy oxygen ions. Furthermore, different proton path lengths through the spray can account for the differences between the 0-degree and 135-degree signal.

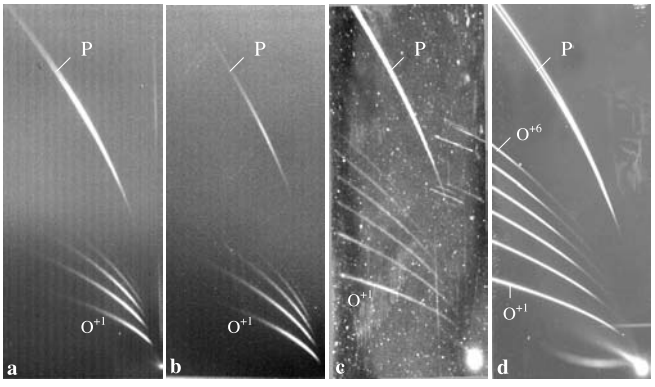

FIGURE 1 Laser (35 fs, $(7 \pm 3) \times 10^{18}$ W/cm^2) produced proton and oxygen–ion traces from water micro-spheres in a spray (**a**, **b** ~ 2000 shot accumulation) and from single large droplets (**c**, **d** $\sim 100\,000$ shot accumulation), observed emission in laser propagation direction (**a**, **c**) and in 135 degree (**b**, **d**) to it; p – denotes the proton traces, the others are O-ion traces of respective charge states (photographs of exposed CR39-plates)

Most importantly, protons have been observed with energies up to 1.5 MeV. These are emitted by objects with a size smaller than the incident laser wavelength. This has never before been observed for cluster-targets. In principle, the water microsphere contains enough molecules to build up, after ionization, an enormous Coulomb potential. Estimating the number of particles in a $d_{sp} = 150$ nm diameter sphere with a particle density of $n_o = 3 \times 10^{22}$ cm^{-3} and assuming a charge state of $Z = 1$ per particle as well as a relative dielectric constant $\varepsilon_r = 1$, one arrives at a sphere potential of $E_{pot} = Ze_o{}^2 d_{sp}{}^2 n_o / 12\varepsilon_o \sim 1$ MeV. This assumes that the respective electrons acquire sufficient kinetic energy to escape from the Coulomb attraction of the ions. In our case, their energy distribution is mainly determined by the ponderomotive potential U_p of the laser: $U_p(\text{eV}) = 9.33 \times 10^{-14} I(\text{W/cm}^2)\lambda^2(\mu\text{m})$. At $\sim 10^{19}$ W/cm^2 and $\lambda = 800$ nm one derives electron energies of ~ 600 keV. This sets an upper limit for the net charge that can build up. The influence of such a potential on the emitted energetic electrons has been observed in experiments with single water droplets [14]. Calculations by Nishihara [18] suggest that at $\sim 10^{19}$ W/cm^2 all electrons can escape from our microsphere, which in the process attains a potential of around 1 MeV. The ion energies we observe are already slightly above this hypothetical limit. Hence, we believe that mere Coulomb repulsion of protons from a charged micro-sphere cannot account for our observations.

The observation of MeV ions expelled from microparticles with sub-wavelength extension gives rise to the the assumption that an essential fraction of them had been exposed to the peak of the pulse before the single 150-nm microdroplets expanded to below critical density. An acceleration mechanism in a rarefied plasma as described by Sarkisov et al. [23] appears unlikely for ultrashort pulses at our intensity. In experiments [23], emission of helium ions with energies up to 6 MeV from laser-heated channels produced with sub-ps pulses at intensities of about 2×10^{19} W/cm^2 in underdense plasmas has been observed perpendicular to the laser propagation. Along the laser propagation no energetic ions have been observed. Because this definitely disagrees with our observations, we can rule out such an acceleration scenario for interpreting our results. Due to the pedestal of the ultrashort pulse, preheating and expansion of target material occur. At a moderate plasma expansion velocity of 10^7 cm/s, the 0.15 μm thick microsphere expands to critical density within 20 ps. Using Ditmire's estimate of the cluster explosion time (1) of [16]) with an electron temperature of ~ 50–1000 eV (derived from X-ray emission at various laser intensities), we infer a disintegration time of the microsphere between 10 and 40 ps. Using low-contrast pulses, few-micron-thin foils failed to yield energetic [10]. In contrast, 3 μm-thick foils [8] with highly contrasted pulses produced copious hot protons. Likewise, Maksimchuk et al. [5] demonstrated 1-MeV proton emission from foils with a thickness below 1 μm irradiated by frequency-doubled laser pulses having enhanced temporal contrast.

Probably, if we had only a single or a few micro-spheres exposed to the laser beam, these would already expand during the pulse pedestal prior to the arrival of the peak intensity of the laser pulse. The essential difference between our spray target and single thin-foil targets lies in the spatial distribution of the former. From the average density ($\sim 10^{11}$ cm^{-3} micro-spheres) and extension (2 mm) [21], one can estimate that each light ray along its path through the spray hits about 100 micro-spheres. Due to the interaction of the pulse–pedestal with the target, the energy of the former can be dissipated by pre-plasma formation in the low-density wing of the spray target and the overall pulse contrast increases, while the pulse continues to travel toward the high-density part of the target. Then, in the inner part of the target, the high-intensity peak of the pulse interacts with micro-spheres that still have an overcritical plasma density. This accounts for the emission of highly energetic ions. The whole process is very delicate: an enhancement of the pedestal level by a factor of 2 . . . 3 completely eliminated the energetic ion emission. The scenario proposed is reminiscent of an "inverse" plasma-mirror effect: The usual plasma mirror reflects high intensities and, thereby, enhances the contrast outside of the plasma. In contrast, here, the pre-plasma diminishes the pedestal and the pulse peak is transmitted up to the region where it can interact as a "high-contrast" pulse with the microspheres. Just how effective particle or cluster clouds can dissipate laser light of moderate intensity, can be also deduced from work where a special "machining" beam [24] is applied to blow away the outer lower-density part of a cluster cloud so as to allow propagation of the main pulse to the its high-density center. Symes et al. [24] found that with such a "machining" beam of about 10^{15} W/cm^2 one can transfer the illuminated part of the cluster cloud into an underdense plasma region with an energy deposition of about 100 mJ per mm so that a high-intensity pulse delayed by 2 ns is not affected and will propagate up to the undisturbed cluster-cloud region. Similarly our pulse pedestal "machines" the target and is consumed in the process.

For the intensities we are applying here, the disintegration of a large cluster or a small spherical object is also governed by the hydrodynamic pressure [16]. This pressure is built up by the hot electron population produced. Hot electrons penetrating the small target and escaping from the surface form a charged double layer, which enables ion acceleration (sheath acceleration or TSNA-mechanism [25], respectively). The majority of hot electrons are trapped by the positive charge, which they are leaving behind. Due to their high energy, they dissipate their energy slowly, and the field survives for several 100 fs. (Proton acceleration up to 1 MeV needs approximately 140 fs in a field of 1 MV/micron.) Because the strength of the field that drives the ion acceleration is a function of the hot-electron density, small objects can build up a sufficiently field, too, provided the object does not disintegrate prior to the arrival of the high-intensity peak of the pulse.

4 Characteristic features of proton spectra

In order to investigate the emitted proton spectra in more detail, single-laser-shot ion spectra were recorded with a MCP-detector instead of the CR-39 plate. An MCP-picture of ion emission in the laser propagation direction and the evaluated spectra of the proton trace are given in Fig. 2. A remarkable modulation in the proton spectrum is obvious, which is different from observations in recent experiments with foil targets for different laser parameters [9, 10]. This appearance of modulations is reproducible. Their detailed structure is subject to fluctuations. This is similar to other experiments [26] where wiggles in the ion spectra were seen, too. However, their modulation depth is at least one order of magnitude smaller than ours. Allen et al. [26] supposed that co-accelerated heavy ions (e.g., carbon or oxygen) give rise to the modulation in the proton spectra and modeled such a scenario. In principle, modulations in ion spectra have already been observed and explained [27] for accelerated ions at laser intensities that were lower by several orders of magnitude. These model calculations have shown that the ion-spectrum modulation occurs upon a certain difference of cold and hot components in the electron energy distribution. For our extremely short pulse, pronounced discontinuities in the electron spectrum are likely. Because we have observed modulations in the proton spectrum already for single large water droplets (cf. Fig. 2), one can conclude that the modulations in the proton spectra from the spray are not entirely generated by superposition. (In a Rayleigh-range of 70 μm times $2w_0 = 6$ μm we have about 200 micro-spheres [21].) The assumption of different electron temperatures could be verified with the help of hard X-ray bremsstrahlung spectra from single large droplets [28]. In the case of the spray, this diagnostic means gives only limited access, because the much smaller microspheres are more transparent for ener-

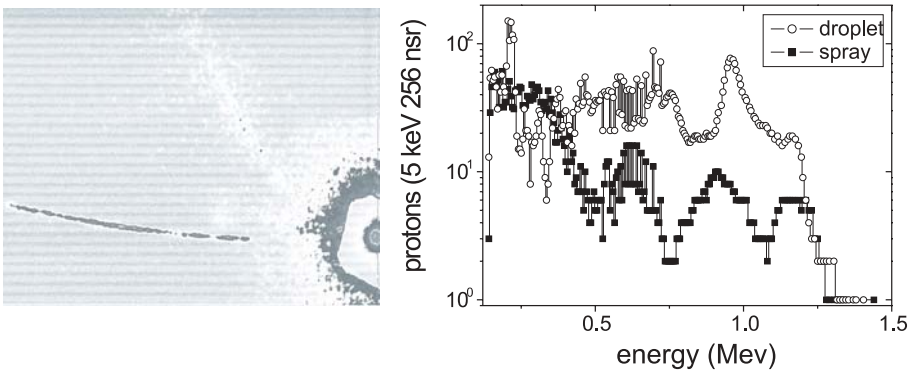

FIGURE 2 Single shot proton spectra in laser propagation direction: Image of a spray-spectrum from the MCP-screen *(left)* and evaluated spectra *(right)* from left trace in comparison to a spectrum of a large droplet

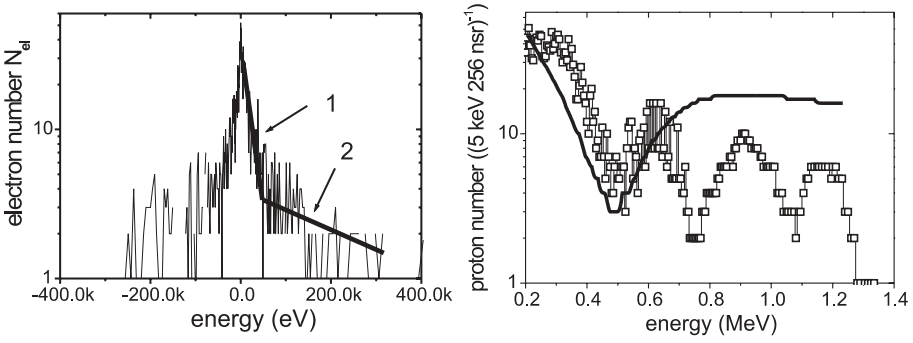

FIGURE 3 *Left*: Electron spectrum from 1 dim LPIC++ code simulation: interaction of a 35 fs, 9×10^{18} W/cm^2 laser pulse with a 150 nm extended hydrogen target at critical electron density (the lines 1 and 2 show two exponential fits corresponding to temperatures of 20 keV and 320 keV; *right*: proton spectrum from the spray (cf. Fig. 2) and simulated spectrum with electron temperature components $T_{\rm cold} = 35$ keV and $T_{\rm hot} = 320$ keV together with a electron density relation of $n_{\rm cold}/n_{\rm hot} = 10$ using a fluid expansion model (cf. description in the text)

getic electrons [21]. Due to a similar laser heating of the microspheres, which is justified by their larger extension compared with the laser skin depth, we can also assume a multicomponent hot electron temperature. Moreover, the result of a one-dimensional particle-in-cell code (LPIC++) shown in Fig. 3 (left) verifies for this small object an electron energy distribution with different temperature components. Further evaluation of ion spectra within the framework of LPIC++ is described by Busch et al. [29]. In Fig. 3 (right) we show how within the fluid-model approach [27] single deep modulations in the spectrum can be simulated. This model can describe a single deep dip in the proton spectrum obtained from large droplets [28], whereas in the case of the spray target the form of the spectra is much more complex and several dips occur (Fig. 3). Due to the presence of a significant number of oxygen ions in different charge states (Fig. 1), it seems possible that a similar mechanism as discussed in [26] is also possible that can explain the modulation in the high-energy tail of the spectra. Superposition effects from different microspheres and the influence of heavy ions on the proton beam have to be investigated further.

5 Summary

In summary, we have demonstrated MeV-proton emission from a spray of water microspheres. We propose that, similar to high-intensity laser interaction with clusters, an essential fraction of the microspheres is exposed to the peak-intensity region of the laser pulse before their disassembly. This is possible because the pedestal of the laser pulse might be lowered during its propagation through the target cloud. This effect needs further experimental verification. If confirmed, highly-energetic-electron-driven explosion of the microspheres can account for the observations.

ACKNOWLEDGEMENTS Acknowledgement: We thank S. Hilscher and U. Jahnke for stimulating discussions and W. Becker for proof-reading the manuscript. The work was partly supported by DFG-project No. 784/6 (S. Busch).

REFERENCES

1 M. Borghesi, S. Bulanov, D.H. Campbell, R.J. Clarke, T.Zh. Esirkepov, M. Galimberti, L.A. Gizzi, A.J. MacKinnon, N.M. Naumova, F. Pegoraro, H. Ruhl, A. Schiavi, O. Willi: Phys. Rev. Lett. **88**, 135 002 (2002)
2 M.I.K. Santala, M. Zepf, F.N. Beg, E.L. Clark, A.E. Dangor, K. Krushelnick, M. Tatarakis, I. Watts, K.W.D. Ledingham, T. McCanny, I. Spencer, A.C. Machacek, R. Allott, R.J. Clarke, P.A. Norreys: Appl. Phys. Lett. **78**, 19 (2001)
3 M. Yamagiwa, J. Koga: J. Phys. D: Appl. Phys. **32**, 2526 (1999)
4 R.A. Snavely, M.H. Key, S.P. Hatchett, T.E. Cowan, M. Roth, T.W. Phillips, M.A. Stoyer, E.A. Henry, T.C. Sangster, M.S. Singh, S.C. Wilks, A. MacKinnon, A. Offenberger, D.M. Pennington, K. Jasuike, A.B. Langdon, B.F. Lasinski, J. Johnson, M.D. Perry, E.M. Campbell: Phys. Rev. Lett. **85**, 2945 (2000)
5 A. Maksimchuk, S. Gu, K. Flippo, D. Umstadter, V.Yu. Bychenkov: Phys. Rev. Lett. **84**, 4108 (2000)
6 A.J. Mackinnon, M. Borghesi, S. Hatchett, M.H. Key, P.K. Patel, H. Campell, A. Schiavi, R. Snavely, S.C. Wilks, O. Willi: Phys. Rev. Lett. **86**, 1769 (2001)
7 J. Badziak, E. Woryna, P. Parys, J. Wolowski, K.Y. Platanov, A.B. Vankov: J. Appl. Phys. **91**, 5504 (2002)
8 A.J. Mackinnon Y. Sentoku, P.K. Patel, D.W. Price, S. Hatchett, M.H. Key, C. Andersen, R. Snavely, R.R. Freeman: Phys. Rev. Lett. **88**, 215 006 (2002)
9 M. Hegelich, S. Karsch, G. Pretzler, D. Habs, K. Witte, W. Guenther, M. Allen, A. Blazevic, J. Fuchs, J.C. Gauthier, M. Geissel, P. Audebert, T. Cowan, M. Roth: Phys. Rev. Lett. **89**,085 002 (2002)
10 I. Spencer, K.W.D. Ledingham, P. McKenna, T. McCanny, R.P. Singhal, P.S. Foster, D. Neely, A.J. Langley, E.J. Divall, C.J. Hooker, R.J. Clarke, P.A. Norreys, E.L. Clark, K. Krushelnick, J.R. Davies: Phys. Rev. E **67**, 046 402 (2003)
11 M. Zepf, E.L. Clark, F.N. Beg, R.J. Clarke, A.E. Dangor, K. Krushelnick, P.A. Norreys, M. Tatarakis, U. Wagner, M.S. Wei: Phys. Rev. Lett. **90**, 064 801 (2003)
12 T. Fujii, Y. Oishi, T. Nayuki, Y. Takizawa, K. Nemoto, T. Kayoiji, K. Horioka, Y. Okano, Y. Hironaka, K.G. Nakamura, Ken-ichi Kondo: Appl. Phys. Lett. **83**, 1524 (2003)
13 K. Matsukado, T. Esirkepov, K. Kinoshita, H. Daido, T. Utsumi, Z. Li, A. Fukumi, Y. Hayashi, S. Orimo, M. Nishiuchi, S.V. Bulanov, T. Tajima, A. Noda, Y. Iwashita, T. Shirai, T. Takeuchi, S. Nakamura, A. Yamazaki, M. Igekami, T. Mihara, A. Morita, M. Uesaka, K. Yoshii, T. Watanabe, T. Hosokai, A. Zhidkov, A. Ogata, Y. Wada, T. Kubota: Phys. Rev. Lett. **91**, 215 001 (2003)
14 S. Busch, S. Ter-Avetisyan, M. Schnürer, M. Kalashnikov, H. Schönnagel, H. Stiel, P.V. Nickles, W. Sandner : Appl. Phys. Lett. **82**, 3354 (2003)
15 S. Karsch, S. Düsterer, H. Schwoerer, F. Ewald, D. Habs, M. Hegelich, G. Pretzler, A. Pukhov, K. Witte, R. Sauerbrey: Phys. Rev. Lett. **91**, 015001 (2003)
16 T. Ditmire T. Donnelly, A.M. Rubenchik, R.W. Falcone, M.D. Perry: Phys. Rev. A **53**, 3379 (1996)
17 M. Lezius, S. Dobosz, D. Normand, M. Schmidt: Phys. Rev. Lett. **80**, 261 (1998)
18 K. Nishihara, H. Amitani, M. Murakami, S.V. Bulanov, T.Zh. Esirkepov: Nucl. Instr. Meth. Phys. Res. A **464**, 98 (2001)
19 R.A. Smith, T. Ditmire, J.W.G. Tisch: Rev. Sci. Instrum. **69,** 3798 (1998)
20 M.P. Kalachnikov, V. Karpov, H. Schönnagel: **12**, 368 (2002)
21 S. Ter-Avetisyan, M. Schnürer, H. Stiel, P.V. Nickles: J. Phys. D: Appl. Phys. **36**, 2421 (2003)
22 A.P. Fews: Nucl. Instrum. Phys. Res. Sect B **72**, 91 (1992)
23 G.S. Sarkisov, V.Yu. Bychenkov, V.N. Novikov, V.T. Tikhonchuk, A. Maksimchuk, S.-Y. Chen, R. Wagner, G. Mourou, D. Umstadter: Phys. Rev. E **59**, 7042 (1999); K. Krushelnik, E.L. Clark, Z. Najmudin, M. Salvati, M.I.K. Santala, M. Tatarakis, A.E. Dangor, V. Malka, D. Neely, R. Allott, C. Danson: Phys. Rev. Lett. **83**, 737 (1999)
24 D.R. Symes, A.J. Comley, J.W.G. Tisch, R.A. Smith: Appl. Phys. Lett. **80**, 4112 (2002)

25 S.P. Hatchett, C.G. Brown, T.E. Cowan, E.A. Henry, J.S. Johnson, M.H. Key, J.A. Koch, A.B. Langdon, B.F. Lasinski, R.W. Lee, A.J. Mackinnon, D.M. Pennington, M.D. Perry, T.W. Phillips, M. Roth, T.C. Sangster, M.S. Singh, R.A. Snavely, M.A. Stoyer, S.C. Wilks, K. Yasuike: Phys. Plasmas **7**, 2076, (2000)
26 M. Allen, Y. Sentoku, P. Audebert, A. Blasevic, T. Cowan, J. Fuchs, J.C. Gauthier, M. Geissel, M. Hegelich, S. Karsch, E. Morse, P.K. Patel, M. Roth: Phys. Plasmas **10**, 3283 (2003); H. Ruhl: University of Nevada, Reno, priv. comm..
27 L.M. Wickens, J.E. Allen: Phys. Rev. Lett. **41**, 243 (1978)
28 S. Ter-Avetisyan, M. Schnürer, S. Busch, P.V. Nickles, W. Sandner: submitted to Phys. Rev. Lett.
29 S. Busch, O. Shiryajev, M. Schnürer, S. Ter-Avetisyan, P.V. Nickles: this issue